Spin-singlet formation in the geometrically frustrated spinel oxide AlV_2O_4: ^{51}V and ^{27}Al NMR measurements

Yasuhiro Shimizu,[1,2] Moe Tanaka,[2] Masayuki Itoh,[2] and Takuro Katsufuji[3]
[1]*Institute for Advanced Research, Nagoya University, Furo-cho, Chikusa-ku, Nagoya 464-8601, Japan*
[2]*Department of Physics, Graduate School of Science, Nagoya University, Furo-cho, Chikusa-ku, Nagoya 464-8602, Japan*
[3]*Department of Physics, Waseda University, Tokyo 169-5551, Japan*
(Received 1 May 2008; revised manuscript received 3 October 2008; published 28 October 2008)

We report ^{51}V and ^{27}Al NMR studies of the spin-frustrated spinel oxide AlV_2O_4 in a temperature range from 850 to 2 K across a structural phase transition at 700 K. Knight shifts and nuclear spin-lattice relaxation rates at the V and Al sites show that the local spin susceptibility at two V sites diminishes at low temperatures in the insulating state, giving direct evidence for the spin-singlet formation. In addition to the singlet spins, one of the two Al sites probes paramagnetic spins with the Curie-Weiss behavior and the spin-glass transition. The results demonstrate coexistence of the spin-singlet cluster and the nearly free spins, anticipated from a theoretical model and the bulk magnetic-susceptibility measurements.

DOI: 10.1103/PhysRevB.78.144423 PACS number(s): 75.50.Ee, 71.30.+h, 76.60.−k, 75.40.Gb

I. INTRODUCTION

Geometrically frustrated antiferromagnets have provided active research fields of many-body quantum phenomena in condensed matter physics. The clear manifestation is emergence of the quantum spin liquid or the resonating valence-bond state in two-dimensional (2D) and three-dimensional (3D) systems. In real materials, however, the degeneracy of singlet spin pairs would be lifted by long-range magnetic order or symmetry breaking of the lattice, often accompanied by the charge and orbital orders. The spin-Peierls transition in one-dimensional (1D) chains with spin $S=1/2$ is an example of the translational symmetry breaking. In contrast to the 1D case, it would not be easy to predict the way of symmetry breaking in 2D and 3D cases, especially in the frustrated lattice. A well-known material is the spinel AB_2O_4 having strong frustration against the spin and charge ordering.[1,2] The spin-singlet formation with the unusual texture emerges accompanied by charge ordering as recently found in $MgTi_2O_4$ (Ref. 3) and $CuIr_2O_4$.[4]

In addition to quantum fluctuations due to geometrical frustration, orbital degrees of freedom are also relevant to the ground-state properties when vanadium atoms occupy the B site in the spinel. Depending on the A-site cations, the system varies from antiferro-orbital orders in $A=$Zn, Mg, and Cd (Refs. 5–8) to a heavy-fermionic metal despite d electron system in $A=$Li.[9] The ground state of AlV_2O_4 also remains to be an attractive issue.[10] The average V valence in AlV_2O_4 is $3d^{2.5}$—the mixed valence ratio, $V^{2+}:V^{3+}=1:1$. The x-ray and electron diffraction measurements showed doubling of the unit cell along the [111] direction at $T_c\sim 700$ K, where the conductivity and magnetic-susceptibility drop.[10,11] The Rietveld analysis of the x-ray diffraction pattern clarified that the low-temperature phase has three inequivalent V sites, named as V1, V2, and V3 in Fig. 1, with the different V-V distances, where the valence of V1 is estimated to be $3+(3d^2)$ based on the V1-O bond length.[11] Hence, the phase transition is regarded as a charge order transition accompanied by a structural distortion and probably by transitions of the spin and orbital states.[10] Here the question is how and why the charge ordering is stabilized in the frustrated lattice. The important experimental facts in the insulator phase are the V-V bond lengths and the anomalous magnetic susceptibility.[11] The V1-V3 bond length (3.039 Å) is considerably longer than those of the V2-V3 (2.809 Å) and nearest V3-V3 (2.610 Å) bonds. The magnetic susceptibility is fitted not only by a Curie-Weiss law with $S=1$ below T_c but needs a singlet-triplet component with $S=1/2$.[11] These results suggest formation of a spin-singlet cluster, called as a

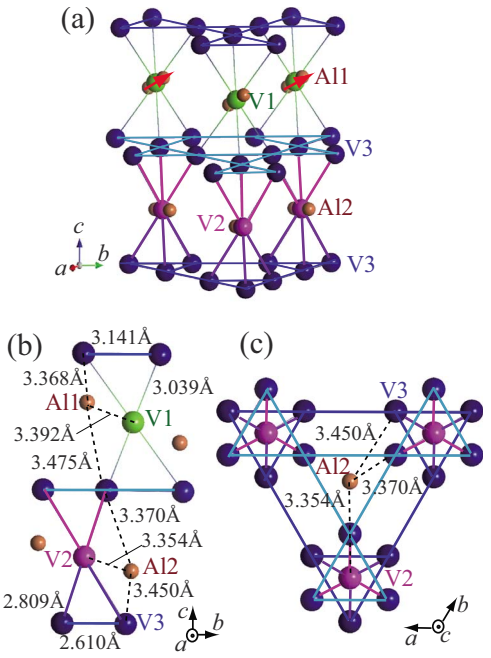

FIG. 1. (Color online) (a) Perspective crystal structure of AlV_2O_4 in the charge ordered state, where O atoms are omitted for clarity. The crystal structures viewed along the (b) a and (c) c axes. The unit cell contains eight V ions with three independent sites, called V1, V2, and V3, sharing 20 valence electrons. The V1 site has the valence V^{3+} with the paramagnetic spin ($S=1$), and the other electrons on the V2 and V3 sites form spin singlets, as clarified in the present NMR studies.

heptamer, consisting of six V3 and one V2 sites, while the origin of the paramagnetic spin susceptibility is attributable to isolated spins $S=1$ on V1.

Theoretical explanation of the spin-singlet heptamer formation was given by Matsuda *et al.*,[12] taking into account the orbital degrees of freedom and the electron correlation. Assuming the isolated heptamer, they concluded that 18 electrons in the heptamer are distributed to two V3 trimers and three V3-V2-V3 bonds, where each V3 trimer and V3-V2-V3 bond share six and two electrons, respectively. However, the confirmation of the spin-singlet state has waited for the direct observation by microscopic magnetic probes since the large paramagnetic spin susceptibility masks the spin-singlet component in the macroscopic measurements.

In this paper, we report NMR detections of local spin susceptibility at the vanadium and aluminum sites on AlV_2O_4 in a wide temperature range, 2–850 K, across T_c =700 K. Observations of the site-dependent Knight shifts provide evidence for the spin-singlet formation as well as the presence of paramagnetic spins following the Curie-Weiss law.

II. EXPERIMENTAL PROCEDURE

The polycrystalline sample of AlV_2O_4 was synthesized by a conventional solid-state reaction method.[10] NMR measurements were performed on the powder sample at magnetic field H of 6.9416 T in a low-temperature T range, 2.3–295 K, and 6.1067 T in a high-T range, 290–850 K, where H was calibrated by measuring ^{51}V NMR of an aqueous $NaVO_3$ solution. NMR spectra were obtained by Fourier transformation (FT) of spin-echo signals which were collected by sweeping frequency with a 200-kHz step. Nuclear spin-lattice relaxation time T_1 was measured at each resonance peak frequency of the V and Al spectra by using the saturation recovery method. The electric quadrupole interaction might split both ^{51}V ($I=7/2$) and ^{27}Al ($I=5/2$) NMR spectra and give non-single-exponential decay of the nuclear magnetization recovery. In the present measurements, however, the quadrupole splitting is negligible in ^{51}V spectra but appears in ^{27}Al spectra below T_c. The FT spin-echo signals at each site showed a single-exponential recovery curve at high temperatures but became non-single-exponential due to the line broadening below 200 K. Then we employed the nuclear spin-lattice relaxation time T_1 of the main component in the double exponential fit.

III. EXPERIMENTAL RESULTS AND DISCUSSION

Figures 2(a) and 2(b) show the temperature dependence of the FT NMR spectra of AlV_2O_4 at 6.9416 T and 6.1067 T, respectively. At 850 K, there are three sharp lines centered at frequencies of 67.80, 68.33, and 69.07 MHz. From the bare gyromagnetic ratio, $^{27}\gamma$=11.094 MHz/T, $^{51}\gamma$ =11.193 MHz/T, and $^{63}\gamma$=11.285 MHz/T, these lines are, respectively, assigned to the resonances of the ^{27}Al and ^{51}V nuclei in the sample and ^{63}Cu in an NMR coil. The smaller intensity of the ^{51}V line than that of the ^{27}Al line stems from

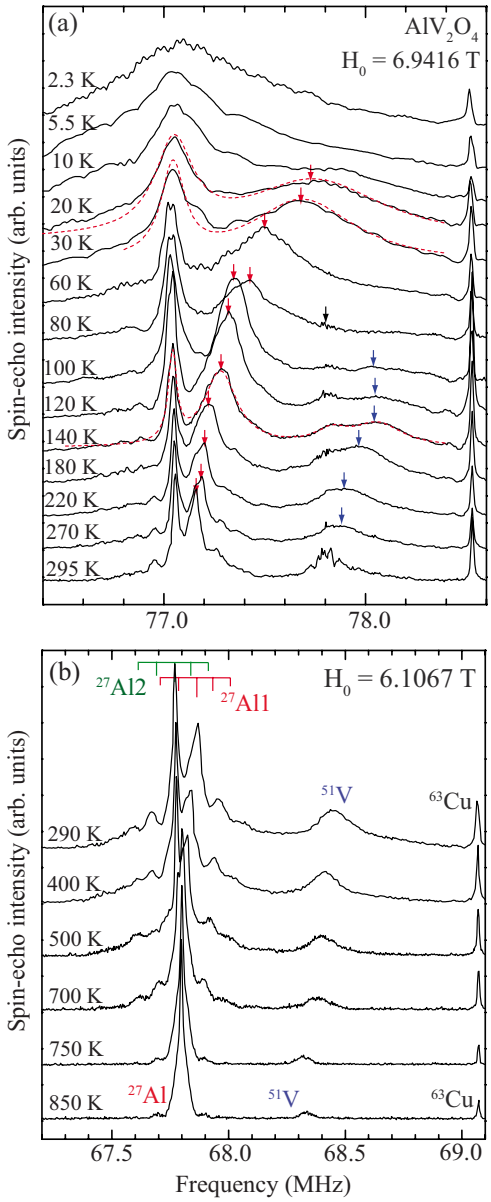

FIG. 2. (Color online) Temperature dependence of the NMR spectra of the powdered sample of AlV_2O_4 (a) below and (b) above the room temperature. The sharp line at 77.8 MHz is from the radio FM broadcast. The red dotted lines are the representative results of the spectral fit by Lorentzians. The downward arrows denote the peak position obtained from the fitting.

the much faster spin-echo decay time T_2 at the ^{51}V site than the $^{27}Al^{3+}$ site without valence electrons—$^{51}T_2$=15 μs and $^{27}T_2$=150 μs at 290 K. At 700 K, the ^{27}Al line splits into two main lines with their satellites, reflecting emergence of two inequivalent Al sites due to the structural phase transition with the unit-cell doubling.[10,11] The nuclear quadrupole splitting manifests appearance of the electric-field gradient due to the distortion of AlO_6 octahedra. The two Al lines at high and low frequencies are reasonably assigned to the signals from Al1 and Al2, respectively, as described later. At the same time, the ^{51}V line jumps into higher frequency and then shows a continuous shift with decreasing temperature. Since the ^{51}V Knight shift, ^{51}K, is dominated by the core polariza-

tion of inner *s* electrons, producing a negative hyperfine field at a nuclear site, the positive shift below 700 K indicates a decrease in the *d* spin susceptibility.

Upon cooling below 290 K, the Al1 line shows a distinct positive shift as seen in Fig. 2(a), while the Al2 line stays nearly the same position, showing a small negative shift. Since the Al^{3+} ion has no on-site electron spin, the hyperfine fields at the Al nuclei come from transferred interactions with *d* electron spins at the V sites. The contrasting temperature dependence of the two Al sites demonstrates that there are both paramagnetic and nonmagnetic V sites, respectively, monitored by Al1 and Al2. Below T_c, we could detect only the nonmagnetic ^{51}V spectrum since the signal from the ^{51}V site with paramagnetic spins would be wiped out due to the large local fields giving the fast T_2. In the observed ^{51}V spectrum below T_c, the expected two V sites, V2 and V3, are not resolved. Then hereafter we define the observed ^{51}V spectrum as "V3" because the V3 site with 6/8 content is the main component of the spectral weight. The spikelike signals staying around 77.8 MHz in Fig. 2(a) are from the FM broadcast and disappear at 6.1067 T in Fig. 2(b). The ^{51}V spectrum continues to move to higher frequency down to 140 K and smears out below 100 K.

At low temperatures below 80 K, the Al1 line broadens with a large positive shift. The broadening is ascribed to the development of inhomogeneous dipole fields from the paramagnetic spins. Below 30 K, the Al2 line also broadens considerably, and the two Al lines merge below 5.5 K. The abrupt appearance of huge inhomogeneous fields at 5.5 K points to the spin-glass transition as observed in the magnetic-susceptibility[10] and specific-heat[13] measurements.

Figure 3 shows the temperature dependence of the ^{51}V and ^{27}Al Knight shifts, ^{51}K and ^{27}K, determined as $K=(\nu_{\rm res}-\nu_0)/\nu_0$, where ν_0 is the resonance frequency calculated from $^{51}\gamma$ and $^{27}\gamma$. Here the resonance frequency $\nu_{\rm res}$ is determined by each peak position of the NMR spectrum above 290 K. At low temperatures, we determined $\nu_{\rm res}$ by fitting the spectra to four Lorentzians for 100–270 K and two Lorentzians below 100 K. The representative fitting results are shown in Fig. 2(a). In vanadium oxides, ^{51}K is generally expressed as a sum of the orbital and spin terms,

$$^{51}K = {}^{51}K^{\rm VV} + {}^{51}K^{\rm spin}, \qquad (1)$$

where $^{51}K^{\rm VV}$ is the *T*-independent Van-Vleck term and $-{}^{51}K^{\rm spin}$ is proportional to the local spin susceptibility, owing to the negative hyperfine coupling constant. Upon cooling from 850 K, $-{}^{51}K$ slightly increases toward T_c at which it drops about 20% and keeps a constant value from 700 to 400 K. The behavior below T_c is fitted by a singlet-triplet model, $-{}^{51}K=-{}^{51}K^{\rm VV}+k_0/[T\{1+\frac{1}{3}\exp(\Delta/k_BT)\}]$, with three fitting parameters, $^{51}K^{\rm VV}=0.47\pm0.03\%$, $k_0=494\pm30$ K, and a spin gap $\Delta=770\pm30$ K. The $^{51}K^{\rm VV}$ value is reasonable for vanadium oxides, e.g., 0.38% in CaV_2O_5 and 0.42% in CaV_3O_7.[14,15] The good fit to the singlet-triplet model applicable to localized spin systems suggests the strong electron localization in the low-*T* insulator phase.

The Knight shifts of the Al1 and Al2 sites, ^{27}K(Al1) and ^{27}K(Al2), stem from transferred hyperfine interactions governed by the transfer path which depends on the Al-O-V bond angle and length. Using the local spin susceptibility at each V site, χ(V1), χ(V2), and χ(V3), in units of emu/V*i*-mol (*i*=1, 2, and 3), ^{27}K(Al1) and ^{27}K(Al2) are expressed as

$$^{27}K(\mathrm{Al1}) = 3A^{(1)}\chi(\mathrm{V1}) + (6A^{(2)} + 3A^{(3)})\chi(\mathrm{V3}), \qquad (2)$$

$$^{27}K(\mathrm{Al2}) = 3A^{(4)}\chi(\mathrm{V2}) + (6A^{(5)} + 3A^{(6)})\chi(\mathrm{V3}), \qquad (3)$$

where $A^{(j)}$ (j=1–6) are the hyperfine coupling constants between Al1-V1, Al1-V3 (3.368 Å), Al1-V3 (3.467 Å), Al2-V2, Al2-V3 (3.450 Å), and Al2-V3 (3.370 Å) in order, as displayed in Fig. 1. As shown in Fig. 3(b), ^{27}K(Al1) is well fitted by the Curie-Weiss law, $^{27}K(\mathrm{Al1})=k_1/(T+\Theta)+k_2$, where k_1 is 52 ± 3 K, the Weiss temperature $\Theta=25\pm4$ K, and $k_2=0.042\pm0.01\%$, using the data in the *T* range, 50–650 K. The broadening of the spectra makes the increasing errors in ^{27}K(Al1) at low temperatures. We plot $1/{}^{27}K$(Al1) against *T* after subtracting k_2 as shown in the inset of Fig. 3(b). The good linearity in the $1/{}^{27}K$(Al1) vs *T* plot in the wide *T* range confirms the validity of the Curie-Weiss fitting and manifests the presence of localized spins coupled with the antiferromagnetic interaction. In contrast, ^{27}K(Al2) decreases below T_c, indicating that the electrons on the V2 site should be nonmagnetic because the V3 site is

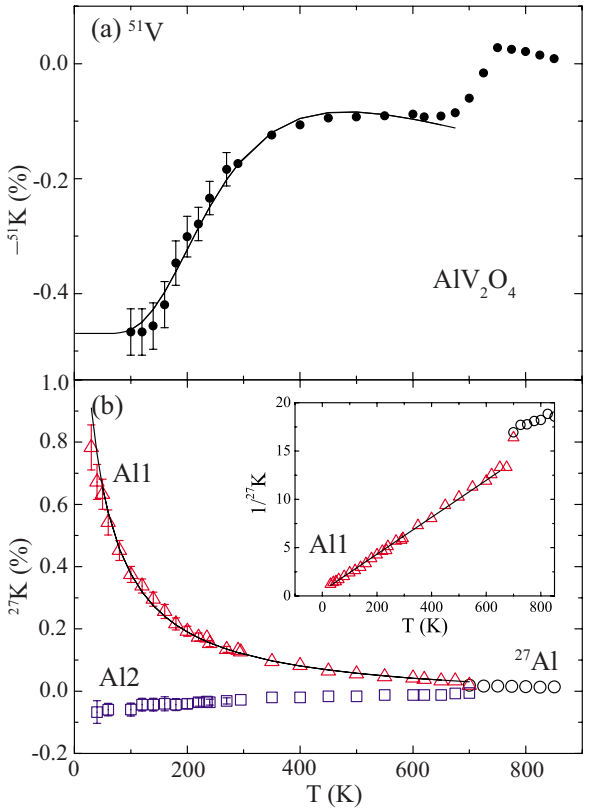

FIG. 3. (Color online) Temperature dependence of the Knight shifts (a) $-{}^{51}K$ and (b) ^{27}K in AlV_2O_4. The solid lines in (a) and (b) are the fitting results by the singlet-triplet model and the Curie-Weiss law, respectively. The inset in (b) is the *T* vs $1/{}^{27}K$ plot, showing the Curie-Weiss behavior with the Weiss temperature of 25 K.

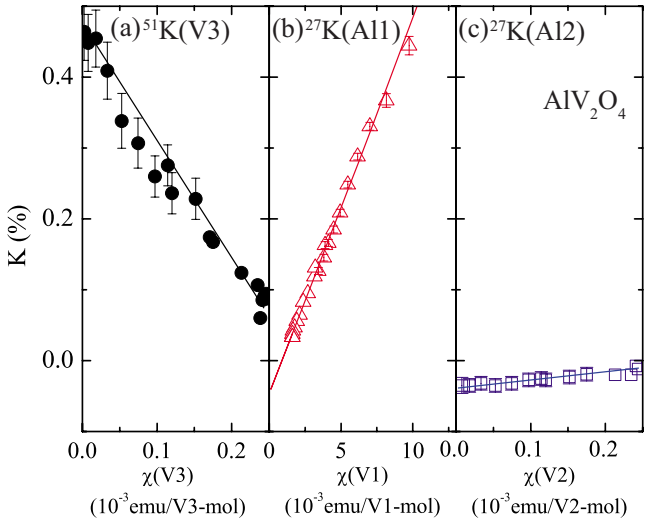

FIG. 4. (Color online) Knight shift versus χ plots for the (a) V3, (b) Al1, and (c) Al2 sites in AlV_2O_4, using the data in a temperature range of 700 to 100 K. The local spin susceptibilities χ(V1), χ(V2), and χ(V3) are expressed as $\chi(\mathrm{V1})=8\chi^{\mathrm{CW}}$ and $\chi(\mathrm{V2})=\chi(\mathrm{V3})=\frac{8}{7}\chi^{\mathrm{ST}}$, where χ^{ST} and χ^{CW} are the calculated magnetic susceptibilities of the singlet-triplet model and the Curie-Weiss law, respectively, using the parameters fitted to the experimental data (Ref. 11).

nonmagnetic as evidenced from ^{51}K. Thus we selectively monitored the paramagnetic local spin susceptibility at the V1 site and the nonmagnetic one at the V2 or V3 site through the ^{51}V and ^{27}Al NMR measurements. Our results provide direct microscopic evidence for the formation of the spin-singlet cluster consisting of the V2 and V3 sites and the coexistence of the paramagnetic spin on the V1 site in AlV_2O_4.

Evaluation of the hyperfine coupling constant may be useful to understand the charge redistribution due to the cluster formation. We plot in Fig. 4 the Knight shifts versus χ(V1), χ(V2), and χ(V3) with T as an implicit parameter. Here the bulk susceptibility χ is expressed by the sum in units of emu/Vi-mol,

$$\chi=\frac{1}{8}\chi(\mathrm{V1})+\frac{1}{8}\chi(\mathrm{V2})+\frac{6}{8}\chi(\mathrm{V3}), \tag{4}$$

where $\chi(\mathrm{V1})=8\chi^{\mathrm{CW}}$ and $\chi(\mathrm{V2})+6\chi(\mathrm{V3})=8\chi^{\mathrm{ST}}$. In the previous report,[11] χ was fitted by the sum of the singlet-triplet component χ^{ST} and the Curie-Weiss component χ^{CW},

$$\chi=\chi^{\mathrm{ST}}+\chi^{\mathrm{CW}}, \tag{5}$$

$$\chi^{\mathrm{ST}}=\frac{D}{T\left\{1+\frac{1}{3}\exp(\Delta/k_{\mathrm{B}}T)\right\}}, \tag{6}$$

$$\chi^{\mathrm{CW}}=\frac{C}{T+\Theta}, \tag{7}$$

using free parameters, $\Delta=844$ K, $\Theta=22.6$ K, $C=0.125$ emu·K/mol, and $D=0.308$ emu·K/mol. When we simply assume $\chi(\mathrm{V2})=\chi(\mathrm{V3})$, ^{51}K below 700 K is written as

$$^{51}K=B\chi(\mathrm{V3})\simeq\frac{8}{7}B\chi^{\mathrm{ST}}. \tag{8}$$

The ^{51}K vs χ(V3) plot in Fig. 4(a) gives the hyperfine coupling constant $B=-82\pm8$ kOe/μ_{B}. This value is comparable to the other vanadium oxides with one valence electron (V^{4+}) such as VO_2 (−85 kOe/μ_{B}) (Ref. 16) but much lower than the two-electron case (V^{3+}) such as V_2O_3 (−140 kOe/μ_{B}) (Ref. 17) despite the average V valence of 2.5+ in AlV_2O_4. In the proposed heptamer model,[12] the valence electrons of V3 are used for two types of singlet pairing—two electrons for the V3-V3 bond and 0.5–1 electron for the V3-V2-V3 bond. Since the V3-V3 bonds with the short-bond length are strong σ bonding and, hence, have a large spin gap, the spin polarization contributing to the hyperfine interaction can be the residual 0.5–1 electron on the V3-V2-V3 bond. In this respect, the obtained small B value is explained by the effective reduction of electron spins involved in the low-energy excitations.

^{27}K(Al1) scales to χ(V1), as seen in Fig. 4(b), but not to the sum of χ(V1) and χ(V3) (not shown). Then ^{27}K(Al1) can be approximately expressed as

$$^{27}K(\mathrm{Al1})\simeq3A^{(1)}\chi(\mathrm{V1})=24A^{(1)}\chi^{\mathrm{CW}}, \tag{9}$$

which yields $A^{(1)}=1.0\pm0.2$ kOe/μ_{B} for $A^{(1)}\gg A^{(2)},A^{(3)}$. Similarly, $A^{(5)}$ and $A^{(6)}$ may be negligible, but the nonmagnetic χ(V2) and χ(V3) terms in Eq. (3) are not distinguishable from Fig. 4(c) and the small difference in the Al2-O-V2/V3 bond lengths and angles (120–124°). The upper and lower limits of $A^{(4)}$ is, respectively, evaluated by fully taking into account or neglecting the Al2-V3 interactions,

$$^{27}K_2\simeq3A^{(4)}\chi(\mathrm{V2})\quad(A^{(4)}\gg A^{(5)}\simeq A^{(6)}), \tag{10}$$

$$\simeq12A^{(4)}\chi(\mathrm{V2})\quad(A^{(4)}\simeq A^{(5)}\simeq A^{(6)}), \tag{11}$$

yielding $0.36\pm0.1<A^{(4)}<1.5\pm0.3$ kOe/μ_{B}.

Figure 5 shows the temperature dependence of $1/T_1$ at the V(V3) and Al(Al1) sites. Here $1/T_1$ is obtained above 100 K for V3 and 20 K for Al1, below which the line merging prevents us from evaluating the reliable T_1 values. $1/T_1$ of ^{51}V drops about 50% at T_c. The large drop compared with ^{51}K is ascribed not only to the change in the spin susceptibility but also to the hyperfine coupling at V3 across T_c due to charge redistribution. After the T-invariant behavior from 700 to 400 K, a characteristic of localized spin system, $1/T_1$ decreases down to 100 K. Absence of an upturn in $1/T_1$ indicates the singlet cluster is not affected by the antiferromagnetic correlation between paramagnetic spins at least above 100 K.

The $1/T_1$ values of the Al1 site are small compared with that of the V site, owing to the small hyperfine coupling. A gradual increase is seen below 200 K down to 10 K, pointing to the development of antiferromagnetic correlation at the V1 site. It is noted that the growth starts far above $\Theta=25$ K. The enhancement of $1/T_1$ is usually seen below the Weiss temperature in the frustrated spin systems such as $LiCrO_2$ and $NiGa_2S_4$.[18,19] The possible reason of the anomalous $1/T_1$ behavior in AlV_2O_4 is the effective reduction in Θ due to the

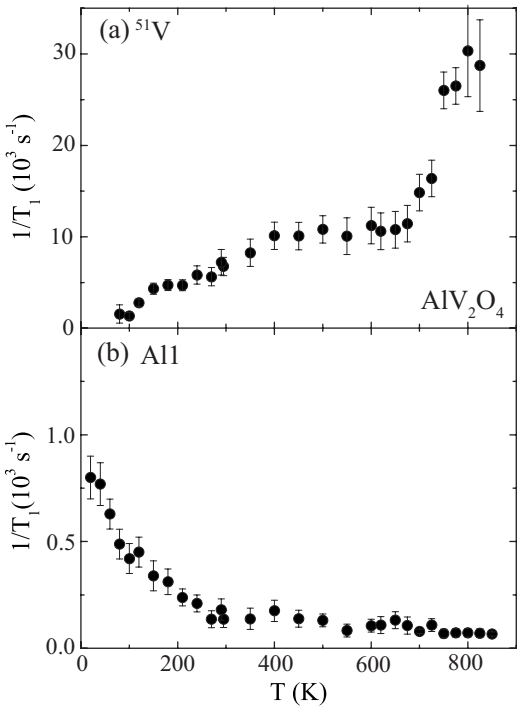

FIG. 5. Temperature dependence of the nuclear spin-lattice relaxation rates at (a) V3 and (b) Al1 sites in AlV_2O_4.

complex magnetic exchange paths between the V1 sites including the direct V1-V1 interactions and the indirect interaction via the spin-singlet cluster.

We thus confirmed that the opening of the spin gap by the cluster formation releases the spin or charge frustration of the spinel structure in AlV_2O_4, with aids of the charge and orbital orders. In the sense that the phase transition accompanies with the translational symmetry breaking, the cluster formation can be classified into the Peierls transition and termed as the orbital-induced Peierls transition,[20] the band Jahn-Teller transition,[21] or the 1D orbital wave ordering,[22] common to the spin dimerization in $MgTi_2O_4$ and the octamer formation in $CuIr_2S_4$.[3,4]

An intriguing unique feature of AlV_2O_4 is that the spin frustration is not completely released but remains on the V1 triangular lattice with the paramagnetic spins exhibiting the spin glass. Here the question is whether the heptamer is robust against the weakly coupled $S=1$ moments on V1. Referring back to the NMR spectra in Fig. 2(a), the Al lines become so broad below 5.5 K and do not resolve the two Al sites. The linewidth measured at 1/10 and 1/2 of the maximum intensity exceeds 2 MHz and 0.5 MHz, respectively. The expected anisotropic dipole fields at Al1 and Al2 from the neighboring 12 V1 sites with randomly orientated magnetic moments are about 6 MHz and 3 MHz in frequency, respectively. Hence the spectral broadening may be explained by the dipole fields from the magnetic V1 sites. It is natural that the much larger energy of the spin gap, 770 K, than the exchange energy between the V1 sites can stabilize the heptamer against the neighboring magnetic moment. However, it would be also possible that the finite antiferromagnetic coupling between the V1 and other V sites induces the tiny magnetic moments on the heptamer.

IV. CONCLUSION

We directly observed the formation of spin singlets in AlV_2O_4 as the decrease in the local spin susceptibility monitored by the ^{51}V and ^{27}Al NMR Knight shifts. The ^{51}V Knight shift behaves as the singlet-triplet model with the spin gap of 770 K. One of the two Al sites showed the Curie-Weiss behavior in the Knight shift with the Weiss temperature of 25 K, while another Al site monitored the nonmagnetic V sites. The results are consistent with the model of the V heptamer located between the magnetic triangular lattice layers.

ACKNOWLEDGMENTS

We thank Y. Motome for fruitful discussion and S. Inoue for technical assistance. This work was financially supported by a Grant-in-Aid for Scientific Research (Grant No. 19014007) and Special Coordination Funds for Promoting Science and Technology (SCF) from the Ministry of Education, Culture, Sports, Science and Technology, Japan, and also by the Grants-in-Aid for Scientific Research (Grants No. 19340097 and No. 19740224) from the Japan Society for the Promotion of Science.

[1] P. W. Anderson, Phys. Rev. **102**, 1008 (1956).
[2] A. P. Ramirez, in *Handbook on Magnetic Materials*, edited by K. J. H. Busch (Elsevier Science, Amsterdam, 2001), Vol. 13, p. 423.
[3] M. Schmidt, W. Ratcliff, P. G. Radaelli, K. Refson, N. M. Harrison, and S. W. Cheong, Phys. Rev. Lett. **92**, 056402 (2004).
[4] P. G. Radaelli, Y. Horibe, M. J. Gutmann, H. Ishibashi, C. H. Chen, R. M. Ibberson, Y. Koyama, Y.-S. Hor, V. Kiryukhin, and S.-W. Cheong, Nature (London) **416**, 155 (2002).
[5] M. Croft, W. Caliebe, H. Woo, T. Tyson, D. Sills, Y. S. Hor, S. W. Cheong, V. Kirykukhin, and S. J. Oh, Phys. Rev. B **67**, 201102(R) (2003).
[6] S.-H. Lee, D. Louca, H. Ueda, S. Park, T. J. Sato, M. Isobe, Y. Ueda, S. Rosenkranz, P. Zschack, J. Iñiguez, Y. Qiu, and R. Osborn, Phys. Rev. Lett. **93**, 156407 (2004).
[7] H. Tsunetsugu and Y. Motome, Phys. Rev. B **68**, 060405(R) (2003); Y. Motome and H. Tsunetsugu, *ibid.* **70**, 184427 (2004).
[8] O. Tchernyshyov, Phys. Rev. Lett. **93**, 157206 (2004).
[9] C. Urano, M. Nohara, S. Kondo, F. Sakai, H. Takagi, T. Shiraki, and T. Okubo, Phys. Rev. Lett. **85**, 1052 (2000).
[10] K. Matsuno, T. Katsufuji, S. Mori, Y. Moritomoto, A. Machida, E. Nishibori, M. Takata, M. Sakata, N. Yamamoto, and H. Takagi, J. Phys. Soc. Jpn. **70**, 1456 (2001).
[11] Y. Horibe, M. Shingu, K. Kurushima, H. Ishibashi, N. Ikeda, K. Kato, Y. Motome, N. Furukawa, S. Mori, and T. Katsufuji, Phys. Rev. Lett. **96**, 086406 (2006); **96**, 169901 (2006).

[12] K. Matsuda, N. Furukawa, and Y. Motome, J. Phys. Soc. Jpn. **75**, 124716 (2006).
[13] K. Matsuno, T. Katsufuji, S. Mori, M. Nohara, A. Machida, Y. Moritomo, K. Kato, E. Nishibori, M. Takata, M. Sakata, K. Kitazawa, and H. Takagi, Phys. Rev. Lett. **90**, 096404 (2003).
[14] T. Ohama, M. Isobe, and Y. Ueda, J. Phys. Soc. Jpn. **69**, 1574 (2000).
[15] H. Iwase, M. Isobe, Y. Ueda, and H. Yasuoka, J. Phys. Soc. Jpn. **65**, 2397 (1996).
[16] K. Takanashi, H. Yasuoka, Y. Ueda, and K. Kosuge, J. Phys. Soc. Jpn. **52**, 3953 (1983).
[17] E. D. Jones, Phys. Rev. **137**, A978 (1965).
[18] L. K. Alexander, N. Büttgen, R. Nath, A. V. Mahajan, and A. Loidl, Phys. Rev. B **76**, 064429 (2007).
[19] H. Takeya, K. Ishida, K. Kitagawa, Y. Ihara, K. Onuma, Y. Maeno, Y. Nambu, S. Nakatsuji, D. E. MacLaughlin, A. Koda, and R. Kadono, Phys. Rev. B **77**, 054429 (2008).
[20] D. I. Khomskii and T. Mizokawa, Phys. Rev. Lett. **94**, 156402 (2005).
[21] Y. Yamashita and K. Ueda, Phys. Rev. Lett. **85**, 4960 (2000).
[22] M. Croft, V. Kiryukhin, Y. Horibe, and S.-W. Cheong, New J. Phys. **9**, 86 (2007).